RESEARCH ARTICLE

MicroRNA regulatory pattern in spinal cord ischemia-reperfusion injury

Zhi-Gang Liu[1], Yin Li[2], Jian-Hang Jiao[1], Hao Long[3], Zhuo-Yuan Xin[4], Xiao-Yu Yang[1, *]

1 Department of Orthopedics, The Second Hospital of Jilin University, Changchun, Jilin Province, China
2 School of Public Health, Jilin University, Changchun, Jilin Province, China
3 Pain Clinic, The Sixth Affiliated Hospital of Xinjiang Medical University, Urumqi, Xinjiang Uygur Autonomous Region, China
4 The Key Laboratory of Zoonosis Search, Chinese Ministry of Education, College of Basic Medicine, Jilin University, Changchun, Jilin Province, China

Funding: *This work was supported by the National Natural Science Foundation of China, No. 81350013 (to XYY).*

Graphical Abstract

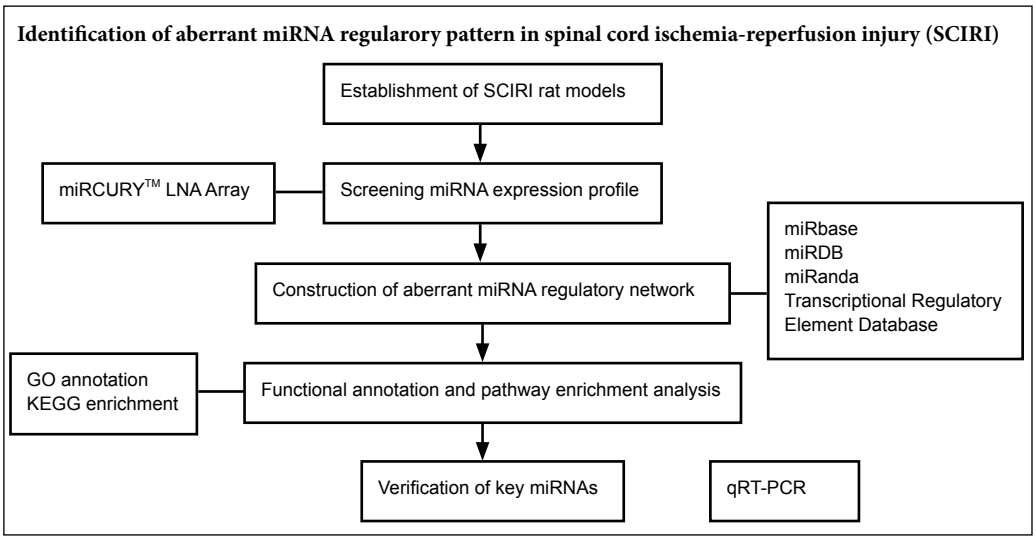

Correspondence to:
Xiao-Yu Yang, PhD,
yangxiaoyu88@sina.com.

orcid:
0000-0003-2516-440X
(Xiao-Yu Yang)

doi: *10.4103/1673-5374.280323*

Received: *July 26, 2019*
Peer review started: *August 1, 2019*
Accepted: *September 10, 2019*
Published online: *May 11, 2020*

Abstract

After spinal cord injury, dysregulated miRNAs appear and can participate in inflammatory responses, as well as the inhibition of apoptosis and axon regeneration through multiple pathways. However, the functions of miRNAs in spinal cord ischemia-reperfusion injury progression remain unclear. miRCURY LNATM Arrays were used to analyze miRNA expression profiles of rats after 90 minutes of ischemia followed by reperfusion for 24 and 48 hours. Furthermore, subsequent construction of aberrantly expressed miRNA regulatory patterns involved cell survival, proliferation, and apoptosis. Remarkably, the mitogen-activated protein kinase (MAPK) signaling pathway was the most significantly enriched pathway among 24- and 48-hour groups. Bioinformatics analysis and quantitative reverse transcription polymerase chain reaction confirmed the persistent overexpression of miR-22-3p in both groups. These results suggest that the aberrant miRNA regulatory network is possibly regulated MAPK signaling and continuously affects the physiological and biochemical status of cells, thus participating in the regulation of spinal cord ischemia-reperfusion injury. As such, miR-22-3p may play sustained regulatory roles in spinal cord ischemia-reperfusion injury. All experimental procedures were approved by the Animal Ethics Committee of Jilin University, China [approval No. 2020 (Research) 01].

Key Words: *gene regulatory networks; microarray analysis; microRNA; miR-22-3p; mitogen-activated protein kinase signaling pathway; nerve regeneration; neural regeneration; spinal cord ischemia-reperfusion injury; transcriptome*

Chinese Library Classification No. *R459.9; R363; R364*

Introduction

Spinal cord ischemia-reperfusion injury (SCIRI), one of the most serious secondary spinal cord injuries, remains an unpredictable and devastating complication in clinical practice, with an incidence of 2–40% (Coselli et al., 2000, 2002). A cascade of secondary damage may be induced by SCIRI, such as neuronal lesions, which leads to further functional loss and behavioral impairments, as well as paraplegia (Bell et al., 2015; Fang et al., 2015). Importantly, there are no efficacious drugs or therapeutic approaches for SCIRI. Thus, many patients suffer substantial physical and psychological consequences. To date, the molecular mechanisms of SCIRI remain unclear, so it is difficult to develop novel drugs or treatments. Thus, it is urgent to identify the molecular mechanisms that underlie the pathogenesis of SCIRI.

Aberrant gene expression is associated with the development of numerous diseases and may involve many types of regulatory molecules. MicroRNA (miRNA) is an important

kind of regulator that functions in RNA silencing and can subsequently regulate gene expression at the post-transcriptional level (Ambros, 2004; Bartel, 2004). miRNAs that remit inflammatory damage to the blood-spinal cord barrier, such as miR-27a, may have essential roles in the progression of SCIRI (Li et al., 2015). Transcription factors (TFs), another important regulator of gene expression at the transcriptional level (Yang et al., 2013), are proteins coded by specific genes that control the transcription rate of other coding genes. Interactions between miRNAs and TFs provide complex information in molecular regulatory patterns. Therefore, alterations in miRNA-TF gene expression regulatory networks may result in the development of SCIRI. Unfortunately, the aberrant miRNA-TF gene regulatory patterns in SCIRI remain unclear. Thus, a systemic analysis of altered miRNA-TF co-regulatory patterns would facilitate understanding of the molecular mechanisms of SCIRI.

This study aimed to analyze miRNA expression profiles and construct a miRNA regulatory pattern in a SCIRI rat model. miRNA expression profiles were analyzed using a miRCURY® LNA® Array (Qiagen, Hilden, Germany). The targets of aberrantly expressed miRNAs were subsequently predicted by integrating the data in three miRNA information databases. Altered miRNA-TF regulatory patterns were constructed based on the Transcriptional Regulatory Element Database (http://rulai.cshl.edu/tred). Gene ontology (GO; http://www.geneontology.org) annotation and Kyoto Encyclopedia of Genes and Genomes (KEGG) pathway enrichment (https://www.kegg.jp) were performed to provide a preliminary analysis of the function of aberrant miRNA-TF patterns in SCIRI, and the main findings were validated by quantitative reverse transcription-polymerase chain reaction (qRT-PCR). The ultimate goal of this study was to provide important clues for future investigations into the molecular mechanisms of SCIRI and facilitate the development of novel therapeutic approaches for this devastating injury.

Materials and Methods

Animals

All experimental procedures were approved by the Animal Ethics Committee of Jilin University, China [approval No. 2020 (Research) 01]. The experimental procedure followed the United States National Institutes of Health Guide for the Care and Use of Laboratory Animals (NIH Publication No. 85-23, revised 1996). Twenty-four male mature Sprague-Dawley rats weighing 220–280 g were purchased from Beijing HFK Bioscience Co., Ltd. [Beijing, China; Animal License No. SCXK (Jing) 2009-0004]. All rats were raised at the School of Public Health at Jilin University, housed in standard cages, and neurologically intact prior to anesthesia. Animals were individually housed after surgery.

SCIRI rat models

To establish SCIRI rat models, 24 clean healthy adult male Sprague-Dawley rats were anesthetized by intraperitoneal injection with 4% sodium pentobarbital (Solarbio Life Science, Beijing, China) at a dose of 50 mg/kg. SCIRI was induced by abdominal aorta occlusion for 90 minutes. Following anesthetization, the abdominal aorta was exposed using a cervicothoracic approach. The abdominal aorta was subsequently cross-clamped between the left renal artery and origin of the right renal artery using non-invasive arterial clips. The occlusion situation was confirmed by detecting beating of the distal abdominal aorta (if clamped successfully, the beating would stop and the color of the left renal would change to dark red). After 90 minutes of ischemia, the arterial clips were removed and reperfusion was allowed to occur for 24 (24-hour group, n = 8) or 48 (48-hour group, n = 8) hours. Sham-operated rats (surgery without abdominal aortic clamp) were used as the control group (n = 8). The Basso Beattie Bresnahan locomotor rating scale was used to evaluate SCIRI rat models (Basso et al., 1995). Sham-operated rats underwent the same procedure without abdominal aortic occlusion.

RNA isolation, microarray hybridization, and signal scanning

Following the establishment of SCIRI rat models, total RNA in lesion tissues was extracted using TRIzol reagent (Invitrogen, Carlsbad, CA, USA) according to the manufacturer's instructions, and then purified with an RNeasy Mini kit (Qiagen). RNA purity and concentration were detected using an UV2800 ultraviolet spectrophotometer (UNICO National, Fairfield, NJ, USA), which required concentrations ranging between 100 ng/mL and 1 mg/mL, an A_{260nm}/A_{280nm} ratio between 1.8 and 2.0, and A_{260nm}/A_{230nm} ratio greater than 1.8.

Following the manufacturer's instructions, miRCURY LNA Array v.16.0 software (Qiagen) was used to profile differentially expressed miRNAs in lesion and normal tissues. Briefly, the extracted total RNA was labeled with a miRCURY Array Power Labeling kit (Qiagen). Labeled total RNAs were subsequently hybridized to the miRCURY LNA Array by incubation at 56°C and rotated at 2 rpm overnight. Fluorescence intensities of the miRCURY LNA Array were scanned using a GenePix 4000B scanner and analyzed with GenePix Pro v.6.0 software (Axon Instruments, Foster City, CA, USA).

MiRNA-TF co-regulatory network analysis

After miRNA expression profile data were obtained, the aberrantly expressed miRNAs with fold changes over 1.5 and P-values less than 0.05 were identified. Regulatory interactions among these differentially expressed miRNAs and target genes were predicted via data integration using miRbase (www.mirbase.org/) (Griffiths-Jones et al., 2006), miRDB (http://mirdb.org) (Wang, 2008), and miRanda (http://www.microrna.org/microrna/home.do) (Betel et al., 2008). TFs were identified based on information provided by the Transcriptional Regulatory Element Database (Zhao et al., 2005). miRNA-TF regulatory patterns were constructed by overlapping these two results, and subsequently visualized using the free software Cytoscape v.3.2.0 (Shannon et al., 2003).

Functional annotation and KEGG pathway enrichment analysis

MiRNA-TF regulatory patterns were identified using The Database for Annotation, Visualization, and Integrated Discovery (https://david.ncifcrf.gov/) (Dennis et al., 2003) and tools in KEGG (Kanehisa and Goto, 2000) to conduct functional annotation and KEGG pathway enrichment analyses. Significantly enriched KEGG pathways were sorted by *P* values less than 0.05.

Quantitative reverse transcription-polymerase chain reaction

The miRNA-TF regulatory patterns identified persistent overexpression of miR-22-3p during SCIRI. qRT-PCR was used to verify expression trends of miR-22-3p. For qRT-PCR, 5 mg of total RNA extracted from lesion and normal spinal cord tissues was reverse-transcribed into cDNA using a first-strand cDNA synthesis kit (Takara, Tokyo, Japan). miRNA expression of rno-miR-22-3p was detected using SYBR Premix Ex Taq (Takara) and an Applied Biosystems 7300 Fast Real-Time PCR System (Foster City, CA, USA). Relative miRNA expression was normalized to U6 expression levels using the comparative $2^{-\Delta\Delta Ct}$ method ($\Delta Ct = Ct_{Target} - Ct_{U6}$, $\Delta\Delta Ct = \Delta Ct_{Lesion} - \Delta Ct_{Normal}$). Primers were designed using Primer Premier software, version 6.0 (Primer Biosoft, Palo Alto, CA, USA) and Primer-BLAST (https://www.ncbi.nlm.nih.gov/tools/primer-blast/). qRT-PCR data were analyzed using Prism Version 5.0 software (GraphPad, San Diego, CA, USA). Rno-miR-22-3p specific primers were 5′-GGT TAA GCT GCC AGT TGA A-3′ (forward, 19 bp) and 5′-CAG TGC GTG TCG TGG AGT-3′ (reverse, 18 bp) (Kang Chen Bio-tech, Shanghai, China). Reaction conditions included a denaturation step at 95°C for 10 minutes, followed by 40 cycles of 95°C for 10 seconds and 60°C for 60 seconds. Primers used to amplify U6 were 5′-GCT TCG GCA GCA CAT ATA CTA AAA T-3′ (forward, 25 bp) and 5′-CGC TTC ACG AAT TTG CGT GTC AT-3′ (reverse, 23 bp) (Kang Chen Bio-tech).

Statistical analysis

Measurement data are expressed as the mean ± SD and were analyzed using R version 3.1.2 software (https://www.r-project.org). All variables were normally distributed, and groups were compared with one-way analysis of variance followed by the least significant difference *post hoc* test. *P*-values < 0.05 were considered statistically significant.

Results

Differentially expressed miRNAs in the lesion region of SCIRI rat models

To identify potential roles of miRNAs in SCIRI, miRNA expression profiles were first detected in SCIRI lesion regions at 24 and 48 hours after reperfusion for comparison with sham-operated tissues. The results demonstrated that among the 695 detected rat miRNAs, at 24 hours, 13 miRNAs were aberrantly expressed, including 12 upregulated miRNAs and 1 downregulated miRNA (**Figure 1A** and **Table 1**). At 48 hours, 105 miRNAs were differentially expressed, including 44 upregulated miRNAs and 61 downregulated miRNAs (**Figure 1B** and **Table 2**). Rno-miR-22-3p was significantly upregulated at both 24 and 48 hours after reperfusion (**Figure 1C**).

Aberrant putative miRNA-TF regulatory patterns in SCIRI rat models

To construct a landscape of miRNA-TF regulatory patterns in SCIRI, the targets of all aberrantly expressed miRNAs were predicted using the miRNA databases miRbase, miRDB, and miRanda (**Additional Table 1**). General miRNA-TF regulatory patterns (**Additional Table 2**) were sequentially built based on rat TF information provided by the Transcriptional Regulatory Element Database (**Additional Table 3**). These networks indicated systemic miRNA-TF regulatory patterns. Furthermore, the regulatory strategies of miRNAs were substantially more complex at 48 hours compared with 24 hours after reperfusion (**Figure 2** and **Additional Figures 1** and **2**). miRNA-TF regulatory patterns indicated the involvement of TFs associated with cell proliferation, survival, and apoptosis, such as Egr2, Stat3, Ets1, Tp53, and Hif-1α. These findings suggest that apoptosis and inflammation may represent important biological processes involved in the progression of SCIRI.

Functional annotation and KEGG pathway enrichment analysis

To determine the function of putative miRNA-TF regulatory patterns, GO gene functional annotation was conducted for all predicted miRNA-target genes. **Figure 3** shows the top 20 significant GO annotation terms that exhibited a significant difference between 24 and 48 hours after reperfusion. Inter-

Table 1 Differentially expressed miRNAs in spinal cords among SCIRI model rats at 24 hours

miRNA	CV value		Fold change	*P*-value
	I/R-24 hours	Sham-24 hours		
Upregulated				
rno-miR-331-5p	0.3349	0.3595	3.115	0.0294
rno-miR-3560	0.1887	0.1173	2.7547	0.0047
rno-miR-463-3p	0.2192	0.2738	2.6625	0.0111
rno-miR-760-5p	0.2326	0.1164	2.0373	0.0212
rno-miR-125b-1-3p	0.0914	0.076	1.8157	0.0015
rno-miR-878	0.211	0.0659	1.7803	0.0239
rno-miR-486	0.2123	0.2746	1.7744	0.0452
rno-miR-22-3p*	0.2149	0.105	1.6759	0.0355
rno-miR-93-5p	0.2351	0.0983	1.6407	0.0494
rno-let-7i-5p	0.1598	0.2717	1.6115	0.0474
rno-miR-134-3p	0.1499	0.2066	1.5131	0.0443
rno-miR-493-5p	0.1086	0.0877	1.5037	0.0093
Downregulated				
rno-miR-3084b-5p	0.2682	0.1679	0.5766	0.0325

Only the miRNAs with fold changes over 3.0 and *P*-value < 0.05 are shown. CV value means coefficient of variation between samples in different groups. *The miRNAs simultaneously differentially expressed in SCIRI rat models at 24 and 48 hours. I/R: Ischemia-reperfusion; SCIRI: spinal cord ischemia-reperfusion injury.

Table 2 Differentially expressed miRNAs in spinal cords among SCIRI model rats at 48 hours

miRNA	CV value		Fold change	*P*-value
	I/R-48 hours	Sham-48 hours		
Upregulated				
rno-miR-935	0.4163	0.4626	17.5851	0.0173
rno-miR-140-5p	0.1901	0.2058	5.9027	0.0017
rno-miR-346	0.2265	0.1888	5.5674	0.0034
rno-miR-873-5p	0.1250	0.5378	5.2567	0.0010
rno-miR-339-5p	0.0464	0.1399	4.6452	0
rno-miR-632	0.3665	0.0658	4.5740	0.0210
rno-miR-149-5p	0.0535	0.3415	4.2643	0.0002
rno-miR-376a-5p	0.3423	0.9216	4.1114	0.0328
rno-miR-330-5p	0.3022	0.4134	3.5261	0.0186
rno-miR-127-3p	0.3104	0.4112	3.4201	0.0212
rno-miR-675-5p	0.2060	0.4406	3.3589	0.0076
rno-miR-22-3p*	0.0282	0.1050	3.2938	0
rno-miR-136-5p	0.1013	0.2865	3.2726	0.0009
Downregulated				
rno-miR-129-2-3p	0.2139	0.4019	0.0569	0.0153
rno-miR-129-1-3p	0.2837	0.3105	0.1008	0.0075
rno-miR-20b-5p	0.3890	0.1709	0.1142	0.0010
rno-miR-130b-3p	0.2840	0.2577	0.1291	0.0044
rno-miR-743a-3p	0.4106	0.1252	0.1356	0.0004
rno-miR-199a-3p	0.8921	0.4862	0.1397	0.0412
rno-miR-497-5p	0.8839	0.1210	0.1442	0.0047
rno-miR-336-5p	0.7635	0.2644	0.1492	0.0069
rno-miR-148a-3p	0.6459	0.1697	0.1722	0.0021
rno-let-7f-5p	0.1446	0.2962	0.1857	0.0090
rno-miR-125b-2-3p	0.4142	0.3197	0.1893	0.0130
rno-miR-28-5p	0.5651	0.1985	0.1897	0.0034
rno-miR-375-5p	0.7981	0.1114	0.2070	0.0023
rno-miR-352	0.1873	0.1367	0.2126	0.0007
rno-miR-19a-3p	0.4423	0.3296	0.2247	0.0175
rno-miR-1188-3p	0.6553	0.1905	0.2350	0.0057
rno-miR-1306-5p	0.6237	0.2748	0.2450	0.0142
rno-miR-182	0.9751	0.2207	0.2450	0.0159
rno-miR-214-3p	1.1334	0.0927	0.2476	0.0116
rno-miR-1839-5p	0.3008	0.3663	0.2523	0.0258
rno-miR-499-5p	0.2286	0.4259	0.2591	0.0406
rno-miR-3547	0.3274	0.2988	0.2599	0.0145
rno-miR-19b-3p	0.6811	0.1261	0.2704	0.0048
rno-miR-98-5p	0.2295	0.0836	0.2990	0.0004
rno-miR-154-3p	0.5108	0.0813	0.3164	0.0028
rno-miR-743b-3p	0.5387	0.3014	0.3199	0.0275
rno-miR-542-5p	0.2353	0.3731	0.3211	0.0366

Only the miRNAs with fold changes over 3.0 and *P*-value < 0.05 are shown. CV value means coefficient of variation between samples in different groups. *The miRNAs simultaneously differentially expressed in SCIRI rat models at 24 and 48 hours. I/R: Ischemia-reperfusion; SCIRI: spinal cord ischemia-reperfusion injury.

estingly, subsequent KEGG enrichment analysis indicated that the mitogen-activated protein kinase (MAPK) signaling pathway was most significantly enriched in both 24- and 48-hour SCIRI groups (**Tables 3** and **4**). This finding indicates that the MAPK signaling pathway may play a critical role during the development of SCIRI and, therefore, represent a potential therapeutic target. Thus, potential correlations were analyzed between differentially expressed miRNAs and the MAPK signaling pathway. All associated miRNA-target genes were mapped to the MAPK signaling pathway (**Figure 4A**), and ideographs were created to demonstrate how these differentially expressed miRNAs regulate MAPK signal transduction processes via MAPK/ERK1/2 (**Figure 4B**), MAPK/p38 (**Figure 4C**), and MAPK/c-JNK (**Figure 4D**).

Verification of findings by qRT-PCR

miRNA-TF regulatory patterns identified in this study were based on miRNA expression profile data. Therefore, qRT-PCR was used to validate rno-miR-22-3p, which was significantly upregulated at both 24 and 48 hours after reperfusion in spinal cord lesion tissues compared with control tissues. qRT-PCR findings were consistent with miRNA expression profile data (**Figure 5**).

Discussion

SCIRI triggers a cascade of molecular alteration events that can lead to neuronal cell death (Juurlink and Sweeney, 1997; White et al., 2000). Inflammation, reactive oxygen species, excitotoxicity (Sattler and Tymianski, 2001), and apoptosis (Gottlieb et al., 1994; Chopp and Li, 1996) are the primary mechanisms involved in SCIRI. To better understand the molecular mechanisms of SCIRI, the current study identified all differentially expressed miRNAs in a rodent model. miRNAs are delicate gene expression regulators with special abilities to regulate the translation and stability of their targets by inhibiting translational activity and promoting target mRNA cleavage (O'Connell et al., 2012; Ksiazek-Winiarek et al., 2013). In view of this fundamental function of miRNAs and their interactions with TFs, miRNAs may act as key regulators in many biological processes in SCIRI, such as apoptosis, cell proliferation, responses to reactive oxygen species, and inflammatory responses. Thus, miRNAs represent potential therapeutic targets for SCIRI.

The current novel findings indicated that miR-22-3p was upregulated at both 24 and 48 hours after reperfusion. miR-22-3p was obviously increased at 48 hours after reperfusion. In myocardial ischemia-reperfusion injury, miR-22 reportedly exhibited anti-apoptosis effects in rats via the downregulation of CREB-binding protein expression, which may decrease the acetylation levels of p53, Bax, and p21 (Yang et al., 2014). MiR-22 overexpression elicits neuroprotection through its targets in general anti-apoptosis signaling pathways, including MAPK/p38 and p53 (Jovicic et al., 2013; Yang et al., 2014). Other differentially expressed miRNAs identified at 24 or 48 hours after reperfusion exhibited a broad range of functions. For example, miR-29c overexpression at 48 hours may exhibit pro-apoptosis effects via the suppression of anti-apoptotic gene expression products (Ye et al., 2010; Armato et al., 2012). miR-451 upregulation at 48 hours may decrease cardiomyocyte death in simulated ischemia-reperfusion injury *in vitro*, as it increases COX-2 expression to protect against cardiac injury (Gray et al., 1990; Penna et al., 2008; Inserte et al., 2009; Zhang et al., 2010). Furthermore, miR-199a targets hypoxia-inducible factor 1α,

Table 3 KEGG pathway enrichment analysis of the predicted miRNA-target genes in the spinal cords of rats 24 hours after ischemia-reperfusioin injury

KEGG terms	Counts	*P* value	Genes
MAPK signaling pathway	14	0.004673737	TGFBR1, MKNK2, PPP3R1, PTPRR, FASLG, PRKX, NRAS, DUSP2, PAK2, RASGRP1, NTRK2, MAP3K8, PLA2G6, MAP3K12
Calcium signaling pathway	11	0.005785292	P2RX4, ADRB3, SLC8A1, ADRB2, P2RX1, CAMK4, PPP3R1, SAE1, VDAC3, PRKX, PTAFR
Axon guidance	8	0.019685239	NRAS, PAK2, LIMK2, LIMK1, SEMA4F, DPYSL5, PPP3R1, CXCL12
Purine metabolism	8	0.048743156	RRM2, NUDT5, PDE11A, GUCY1B3, ENTPD3, AMPD3, PRPS2, POLR3D
Adipocytokine signaling pathway	7	0.003087337	SLC2A4, NFKBIE, SLC2A1, PRKAB1, ACSL4, CAMKK1, STAT3
Neurotrophin signaling pathway	7	0.054806488	NRAS, YWHAG, CAMK4, NFKBIE, NTRK2, FASLG, SH2B3
PPAR signaling pathway	6	0.018280307	SCD1, OLR1, EHHADH, APOA5, GK, ACSL4
Apoptosis	6	0.036347469	CASP8, PPP3R1, PDE11A, FASLG, BCL2L1, PRKX
T cell receptor signaling pathway	6	0.086662229	NRAS, PAK2, NFKBIE, RASGRP1, MAP3K8, PPP3R1
Renal cell carcinoma	5	0.06160854	NRAS, PAK2, VHL, SLC2A1, EGLN3

Table 4 KEGG pathway enrichment analysis of the predicted miRNA-target genes in the spinal cords of rats 48 hours after ischemia-reperfusioin injury

KEGG terms	Counts	*P* value	Genes
Pathways in cancer	68	1.20E-04	FGF9, ARNT2, PPARG, TGFB3, FASLG, FGF13, TGFB2, PAX8, CASP8, SLC2A1, MYC, EGFR, RET, CTBP1, CTBP2, HSP90AA1, RALBP1, RELA, TP53, VEGFB, HIF1A, CRKL, PIAS3, NCOA4, MAPK3, MAPK9, PDGFRB, BID, WNT5A, XIAP, ERBB2, EGLN3, KITLG, TFG, CDH1, KIT, BCL2L1, TPM3, IGF1R, PTK2, LAMB2, NKX3-1, RUNX1, AXIN2, FIGF, PIK3R2, FN1, CSF1R, MAP2K1, VHL, TGFBR1, FZD1, IGF1, RAF1, SMAD2, STAT1, STAT3, DVL1, NRAS, CBLB, CDKN1B, HDAC1, GSK3B, RASSF1, NTRK1, MTOR, IKBKB, CRK
MAPK signaling pathway	51	0.010601308	FGF9, GNA12, TGFB3, FASLG, FGF13, PRKX, TGFB2, BDNF, MAP3K8, PAK1, MYC, EGFR, RELA, TP53, PTPRR, CRKL, ARRB2, RRAS2, MAPK3, PLA2G6, PDGFRB, MAPK9, MAP3K12, TNF, MRAS, MAPKAPK3, MKNK2, CACNB1, PPP3R1, CACNB2, CACNB3, PPM1B, RASGRP1, MAP2K1, NTF3, TGFBR1, RAF1, DUSP5, NRAS, DUSP2, MAPK13, NTRK1, MAPK14, NTRK2, RAP1A, MAPK8IP1, CACNA1C, IKBKB, CRK, CD14, CACNA1B
Chemokine signaling pathway	45	1.54E-05	CXCL1, ADCY3, GNAI3, GNAI2, ADCY5, BCAR1, ADCY6, GNG11, CX3CL1, CXCR3, CXCL12, PRKX, PXN, CCL7, CXCL10, CCL22, PTK2, PLCB4, PAK1, CSK, GNG5, PIK3R2, MAP2K1, HCK, RELA, RAF1, STAT1, PRKCD, STAT3, STAT2, CCL11, NRAS, CRKL, CCR5, AGTR1B, ARRB2, CXCL13, GNG10, GSK3B, MAPK3, GRK6, RAP1A, GRK5, IKBKB, CRK
Regulation of actin cytoskeleton	41	0.015774407	ITGAL, FGF9, BCAR1, MRAS, WASF1, GNA12, PIP5K1B, ITGB4, FGF13, ARPC5, BDKRB2, PXN, PFN1, PTK2, PFN2, EZR, PAK1, CSK, FN1, PIK3R2, EGFR, MAP2K1, LIMK2, LIMK1, MYLK2, RAF1, PPP1CC, PPP1CB, NRAS, CRKL, CHRM3, CHRM2, RRAS2, CFL1, MAPK3, F2, ITGA7, PDGFRB, CRK, CD14, MYH10
Neurotrophin signaling pathway	37	7.71E-06	YWHAZ, FASLG, BDNF, NGFRAP1, CSK, ARHGDIA, PIK3R2, IRAK2, PDK1, IRS3, NTF3, MAP2K1, RELA, TP53, YWHAB, RAF1, PRKCD, IRS1, YWHAE, NRAS, YWHAG, CRKL, YWHAH, CAMK4, MAPK13, NTRK1, GSK3B, MAPK14, MAPK3, NTRK2, YWHAQ, RAP1A, MAPK9, NGFR, IKBKB, CRK, CALM1
Insulin signaling pathway	36	5.89E-05	PRKAG1, PRKAG2, MKNK2, RHOQ, PRKX, PRKAR2A, EIF4EBP1, PPP1R3B, SLC2A4, PRKAA2, INSR, PIK3R2, IRS3, MAP2K1, FLOT2, FLOT1, PRKAB1, RAF1, FBP2, PPP1CC, IRS1, PPP1CB, PCK1, NRAS, CBLB, CRKL, EIF4E, PYGL, GSK3B, MAPK3, MAPK9, MTOR, PTPN1, IKBKB, CRK, CALM1
Oocyte meiosis	29	7.62E-04	ADCY3, YWHAZ, PPP2R5B, ADCY5, BTRC, ADCY6, PPP3R1, PRKX, IGF1R, PPP2CA, PPP2CB, STAG3, PPP2R1B, PPP2R1A, MAP2K1, YWHAB, IGF1, SKP1, PPP1CC, PPP1CB, YWHAE, CCNB1, YWHAG, CCNB2, YWHAH, PLK1, MAPK3, YWHAQ, CALM1
Lysosome	29	0.001817144	CLTA, CLTB, ATP6AP1, HEXA, PPT2, ABCA2, ACP2, CLTC, CTSL1, ASAH1, SLC11A2, AP3M1, SCARB2, ATP6V0D1, ABCB9, LAPTM4A, LIPA, PLA2G15, PSAP, CD164, M6PR, GNS, SLC17A5, LAMP3, IGF2R, CTSE, CTSB, GGA1, CTSH
Cell adhesion molecules	29	0.044450344	CLDN8, PVR, ITGAL, MPZL1, CLDN9, CLDN3, CDH1, L1CAM, CLDN11, SDC2, RT1-DA, NRCAM, ALCAM, PVRL2, ESAM, CD4, NEGR1, CD28, SELL, NFASC, CD276, NLGN3, CD40, NCAM1, NCAM2, SDC1, CLDN1, CNTN2, SELE
Vascular smooth muscle contraction	27	0.004616772	ADCY3, ADORA2B, ADCY5, CALD1, ADCY6, GNA12, PRKX, PLCB4, CYP4A8, RAMP1, RAMP2, ACTC1, MAP2K1, PRKCH, RAF1, MYLK2, PPP1CC, PRKCE, PPP1CB, PRKCD, AGTR1B, MAPK3, PLA2G6, GUCY1B3, CACNA1C, ADRA1D, CALM1

which in turn, stabilizes the pro-apoptotic TF p53. Thus, the observed decrease of miR-199a at 48 hours in this study may prevent ischemia-reperfusion injury in the heart, kidney, and any other tissues (Rane et al., 2009; Wang et al., 2014; Bi et al., 2015; Nanayakkara et al., 2015). However, the functions of many other differentially expressed miRNAs identified in this study have not been previously reported and, thus, require further investigation.

The MAPK signaling pathway reportedly plays essential roles in responding to external stimuli during isch-

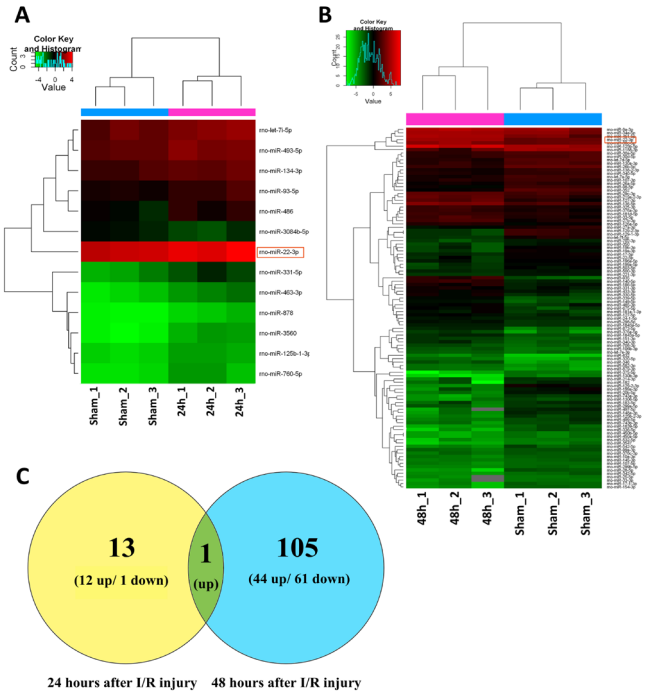

Figure 1 Cluster analyses of altered miRNAs after SCIRI.
(A) Aberrantly expressed miRNAs in SCIRI and sham-operated tissues at 24 hours (n = 3). (B) Aberrantly expressed miRNAs in SCIRI and sham-operated tissues at 48 hours post-injury (n = 3). Each row represents an individual miRNA, and each column represents a sample. Red represents relatively high expression level, while green represents relatively low expression. (C) Number of aberrantly expressed miRNAs in the spinal cord lesion regions following reperfusion: overlapping regions between the ovals indicate the number of differentially expressed miRNAs shared at 24 and 48 hours after reperfusion. SCIRI: Spinal cord ischemia-reperfusion injury.

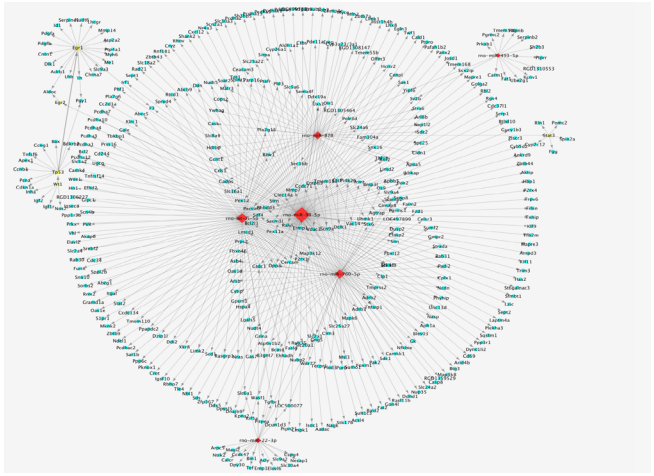

Figure 2 Putative miRNA-TF regulatory patterns in spinal cord ischemia-reperfusion injury.
Blue circles represent miRNA-target genes (all node details are provided in Additional Tables 1–3). Yellow triangles represent TFs. Red diamonds represent differentially expressed miRNAs with predicted target genes. This is a landscape of putative miRNA-TF regulatory patterns at 24 hours after reperfusion in which the miRNAs were upregulated. TF: Transcription factor.

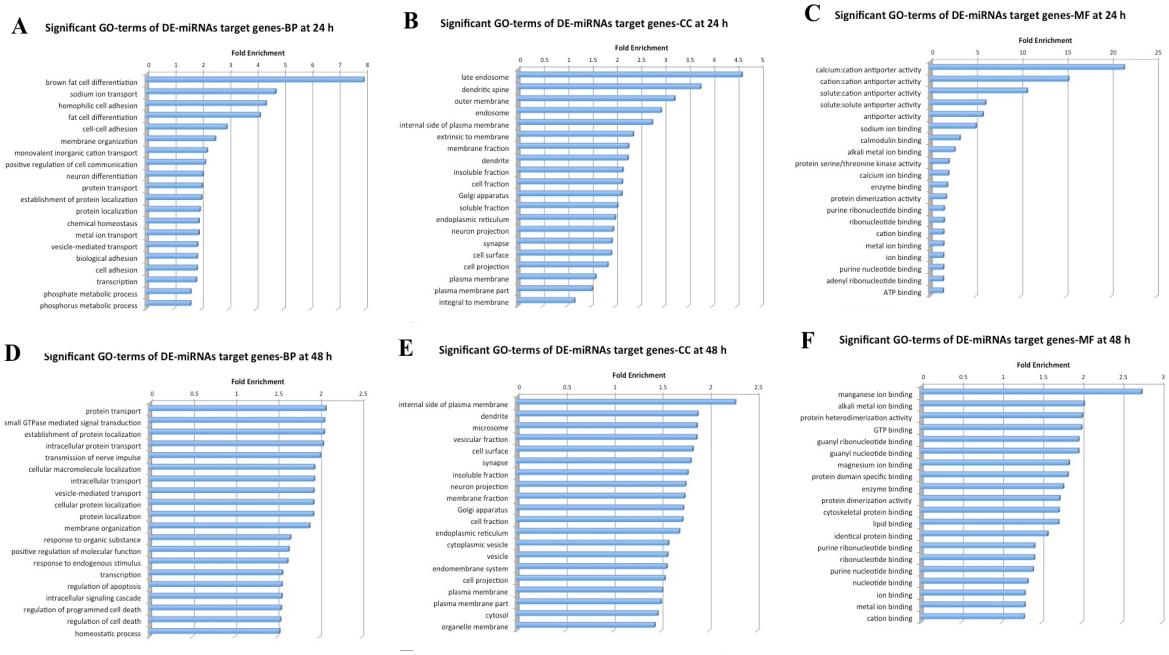

Figure 3 GO annotation of all predicted target genes.
(A–C) Biological Process (BP), Cell Component (CC), and Molecular Function (MF) terms, respectively, of all miRNA-target genes in the 24-hour group. (D–F) BP, CC, and MF terms, respectively, of all miRNA-target genes in the 48-hour group. Only the top 20 significantly enriched GO terms are presented. DE: Differentially expressed.

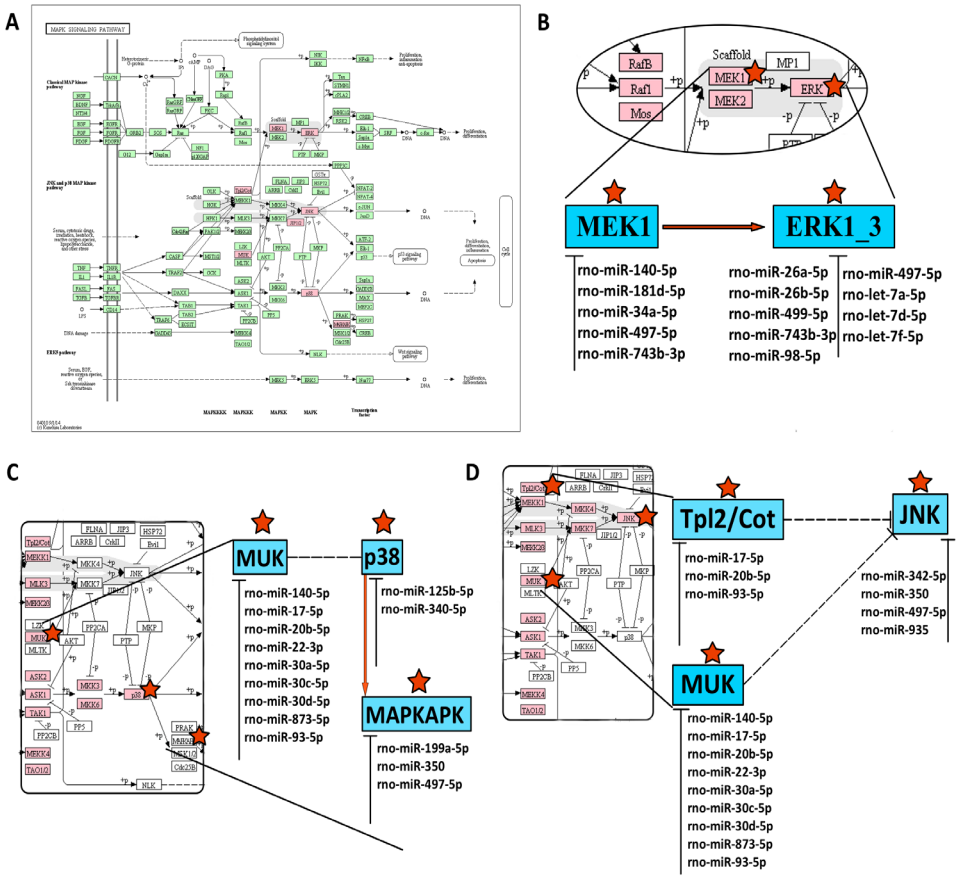

Figure 4 Potential correlations between differentially expressed miRNAs and MAPK pathways related to SCIRI.
(A) Map of predicted miRNA-target genes in the MAPK signaling pathway; mapped genes are indicated by pink rectangles. (B) Detailed putative miRNA regulatory pattern in the MAPK/ERK1/2 signaling pathway. (C) Detailed putative miRNA regulatory pattern in the MAPK/p38 signaling pathway. (D) Detailed putative miRNA regulatory pattern in the MAPK/JNK signaling pathway. ERK: Extracellular-signal-related kinase; JNK: c-Jun N-terminal kinase; MAPK: mitogen-activated protein kinase; SCIRI: spinal cord ischemia-reperfusion injury.

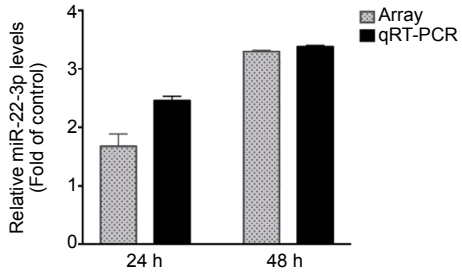

Figure 5 qRT-PCR analysis confirmed the microarray detection of key miRNAs aberrantly expressed at both 24 and 48 hours after SCIRI.
Relative expression represents the change in expression compared with the control group at 24 or 48 hours after reperfusion. Data are expressed as the mean ± SD (n = 3). qRT-PCR results confirmed miR-22-3p expression levels detected by microarray. qRT-PCR: Quantitative reverse transcription-polymerase chain reaction.

emia-reperfusion. ERK1/2, JNK, and p38 are three major signaling cascades in the MAPK signaling transduction pathway. MAPK/ERK1/2 activates ERK1/2 and exhibits a close relationship with cell survival, differentiation, and proliferation based on the association with neurotropic factors, which are also involved in myocardial ischemia-reperfusion injury (Boulton et al., 1991; Segal and Greenberg, 1996; Jiang et al., 2013). Nuclear factor-κB is induced through the MAPK/ERK1/2 signaling pathway to regulate anti-apoptotic mechanisms in SCIRI lesion tissues (Lu et al., 2010). Furthermore, MAPK/p38/JNK is regarded as a stress-induced kinase and plays important roles in inflammatory responses (Wang et al., 2009; Abi-Hachem et al., 2010). In this study, at 24 and 48 hours after ischemia-reperfusion, most of the predicted differentially expressed miRNA target genes were mapped to the MAPK signaling pathway (14 at 24 hours and 51 at 48 hours). These findings indicate that although the molecular mechanisms of SCIRI are complicated and remain unclear, MAPK appears to be the most critical signaling pathway. And miR-22-3p may affect SCIRI process by regulating MAPK pathway.

Despite these promising findings, there are several limitations that must be considered in the interpretation of our results. First, only three repetitions were performed for each group, which may have resulted in uncontrollable errors. Second, the current study only involved a preliminary analysis of the functions of putative miRNA-TF regulatory patterns, which require further validation by functional experiments.

Nevertheless, to the best of our knowledge, this study is the first to develop a general landscape of aberrant miRNA-TF regulatory patterns in a SCIRI model. These novel findings provide important clues for future studies on SCIRI and a theoretical foundation for the development of novel therapeutic approaches.

Acknowledgments: *We would like to thank the School of Public Health, Jilin University for providing the Sprague-Dawley rats and animal surgical equipment.*

Author contributions: *Study design: ZGL; study implementation: ZYX, YL, JHJ and HL; data analysis: ZYX and ZGL; sample collection: YL and HL; manuscript writing: ZGL; manuscript reviewing: XYY. All authors approved the final version of the paper.*
Conflicts of interest: *The authors declare that there are no conflicts of interest associated with this manuscript.*
Financial support: *This work was supported by the National Natural Science Foundation of China, No. 81350013 (to XYY). The funding source had no role in study conception and design, data analysis or interpretation, paper writing or deciding to submit this paper for publication.*
Institutional review board statement: *All experimental procedures were approved by the Animal Ethics Committee of Jilin University, China [approval No. 2020 (Research) 01]. The experimental procedure followed the United States National Institutes of Health Guide for the Care and Use of Laboratory Animals (NIH Publication No. 85-23, revised 1996).*

Data sharing statement: *Datasets analyzed during the current study are available from the corresponding author on reasonable request.*
Plagiarism check: *Checked twice by iThenticate.*
Peer review: *Externally peer reviewed.*

Additional files:

Additional Figure 1: *Putative miRNA-TF regulatory patterns in SCIRI for up-regulated miRNAs in the 48-hour group.*

Additional Figure 2: *Putative miRNA-TF regulatory patterns in SCIRI for down-regulated miRNAs in the 48-hour group.*

Additional Table 1: *Information for miRNA target genes.*

Additional Table 2: *Pattern details.*

Additional Table 3: *Transcription factors (TFs) information.*

References

Abi-Hachem RN, Zine A, Van De Water TR (2010) The injured cochlea as a target for inflammatory processes, initiation of cell death pathways and application of related otoprotectives strategies. Recent Pat CNS Drug Discov 5:147-163.

Ambros V (2004) The functions of animal microRNAs. Nature 431:350-355.

Armato J, DeFronzo RA, Abdul-Ghani M, Ruby R (2012) Successful treatment of prediabetes in clinical practice: targeting insulin resistance and beta-cell dysfunction. Endocr Pract 18:342-350.

Bartel DP (2004) MicroRNAs: genomics, biogenesis, mechanism, and function. Cell 116:281-297.

Basso DM, Beattie MS, Bresnahan JC (1995) A sensitive and reliable locomotor rating scale for open field testing in rats. J Neurotrauma 12:1-21.

Bell MT, Puskas F, Bennett DT, Cleveland JC Jr, Herson PS, Mares JM, Meng X, Weyant MJ, Fullerton DA, Brett Reece T (2015) Clinical indicators of paraplegia underplay universal spinal cord neuronal injury from transient aortic occlusion. Brain Res 1618:55-60.

Betel D, Wilson M, Gabow A, Marks DS, Sander C (2008) The microRNA.org resource: targets and expression. Nucleic Acids Res 36:D149-153.

Bi LY, Zhao DA, Yang DS, Guo JG, Liang B, Zhang RX, Zhao JL, Bai HT, Li SJ (2015) Effects of autologous SCF- and G-CSF-mobilized bone marrow stem cells on hypoxia-inducible factor-1 in rats with ischemia-reperfusion renal injury. Genet Mol Res 14:4102-4112.

Boulton TG, Nye SH, Robbins DJ, Ip NY, Radziejewska E, Morgenbesser SD, DePinho RA, Panayotatos N, Cobb MH, Yancopoulos GD (1991) ERKs: a family of protein-serine/threonine kinases that are activated and tyrosine phosphorylated in response to insulin and NGF. Cell 65:663-675.

Chopp M, Li Y (1996) Apoptosis in focal cerebral ischemia. Acta Neurochir Suppl 66:21-26.

Coselli JS, LeMaire SA, Conklin LD, Koksoy C, Schmittling ZC (2002) Morbidity and mortality after extent II thoracoabdominal aortic aneurysm repair. Ann Thorac Surg 73:1107-1116.

Coselli JS, LeMaire SA, Miller CC, 3rd, Schmittling ZC, Koksoy C, Pagan J, Curling PE (2000) Mortality and paraplegia after thoracoabdominal aortic aneurysm repair: a risk factor analysis. Ann Thorac Surg 69:409-414.

Dennis G, Jr., Sherman BT, Hosack DA, Yang J, Gao W, Lane HC, Lempicki RA (2003) DAVID: database for annotation, visualization, and integrated discovery. Genome Biol 4:P3.

Fang B, Li XQ, Bi B, Tan WF, Liu G, Zhang Y, Ma H (2015) Dexmedetomidine attenuates blood-spinal cord barrier disruption induced by spinal cord ischemia reperfusion injury in rats. Cell Physiol Biochem 36:373-383.

Gottlieb RA, Burleson KO, Kloner RA, Babior BM, Engler RL (1994) Reperfusion injury induces apoptosis in rabbit cardiomyocytes. J Clin Invest 94:1621-1628.

Gray GJ, Kaul R, Sherburne R, Wenman WM (1990) Detection of the surface-exposed 18-kilodalton binding protein in Chlamydia trachomatis by immunogold staining. J Bacteriol 172:3524-3528.

Griffiths-Jones S, Grocock RJ, van Dongen S, Bateman A, Enright AJ (2006) miRBase: microRNA sequences, targets and gene nomenclature. Nucleic Acids Res 34:D140-144.

Inserte J, Molla B, Aguilar R, Traves PG, Barba I, Martin-Sanz P, Bosca L, Casado M, Garcia-Dorado D (2009) Constitutive COX-2 activity in cardiomyocytes confers permanent cardioprotection Constitutive COX-2 expression and cardioprotection. J Mol Cell Cardiol 46:160-168.

Jiang M, Wang L, Jiang HH (2013) Role of spinal MAPK-ERK signal pathway in myocardial ischemia-reperfusion injury. Zhongguo Dang Dai Er Ke Za Zhi 15:387-391.

Jovicic A, Zaldivar Jolissaint JF, Moser R, Silva Santos Mde F, Luthi-Carter R (2013) MicroRNA-22 (miR-22) overexpression is neuroprotective via general anti-apoptotic effects and may also target specific Huntington's disease-related mechanisms. PLoS One 8:e54222.

Juurlink BH, Sweeney MI (1997) Mechanisms that result in damage during and following cerebral ischemia. Neurosci Biobehav Rev 21:121-128.

Kanehisa M, Goto S (2000) KEGG: kyoto encyclopedia of genes and genomes. Nucleic Acids Res 28:27-30.

Ksiazek-Winiarek DJ, Kacperska MJ, Glabinski A (2013) MicroRNAs as novel regulators of neuroinflammation. Mediators Inflamm 2013:172351.

Li XQ, Lv HW, Wang ZL, Tan WF, Fang B, Ma H (2015) MiR-27a ameliorates inflammatory damage to the blood-spinal cord barrier after spinal cord ischemia: reperfusion injury in rats by downregulating TICAM-2 of the TLR4 signaling pathway. J Neuroinflammation 12:25.

Lu K, Liang CL, Liliang PC, Yang CH, Cho CL, Weng HC, Tsai YD, Wang KW, Chen HJ (2010) Inhibition of extracellular signal-regulated kinases 1/2 provides neuroprotection in spinal cord ischemia/reperfusion injury in rats: relationship with the nuclear factor-kappaB-regulated anti-apoptotic mechanisms. J Neurochem 114:237-246.

Nanayakkara G, Alasmari A, Mouli S, Eldoumani H, Quindry JC, McGinnis G, Fu X, Berlin A, Peters B, Zhong J, Amin RH (2015) Cardioprotective HIF-1alpha-frataxin signaling against ischemia-reperfusion injury. Am J Physiol Heart Circ Physiol 309:H867-879.

O'Connell RM, Rao DS, Baltimore D (2012) microRNA regulation of inflammatory responses. Annu Rev Immunol 30:295-312.

Penna C, Mancardi D, Tullio F, Pagliaro P (2008) Postconditioning and intermittent bradykinin induced cardioprotection require cyclooxygenase activation and prostacyclin release during reperfusion. Basic Res Cardiol 103:368-377.

Rane S, He M, Sayed D, Vashistha H, Malhotra A, Sadoshima J, Vatner DE, Vatner SF, Abdellatif M (2009) Downregulation of miR-199a derepresses hypoxia-inducible factor-1alpha and Sirtuin 1 and recapitulates hypoxia preconditioning in cardiac myocytes. Circ Res 104:879-886.

Sattler R, Tymianski M (2001) Molecular mechanisms of glutamate receptor-mediated excitotoxic neuronal cell death. Mol Neurobiol 24:107-129.

Segal RA, Greenberg ME (1996) Intracellular signaling pathways activated by neurotrophic factors. Annu Rev Neurosci 19:463-489.

Shannon P, Markiel A, Ozier O, Baliga NS, Wang JT, Ramage D, Amin N, Schwikowski B, Ideker T (2003) Cytoscape: a software environment for integrated models of biomolecular interaction networks. Genome Res 13:2498-2504.

Wang L, Zhang L, Chen ZB, Wu JY, Zhang X, Xu Y (2009) Icariin enhances neuronal survival after oxygen and glucose deprivation by increasing SIRT1. Eur J Pharmacol 609:40-44.

Wang T, Zhou YT, Chen XN, Zhu AX (2014) Putative role of ischemic postconditioning in a rat model of limb ischemia and reperfusion: involvement of hypoxia-inducible factor-1alpha expression. Braz J Med Biol Res 47:738-45.

Wang X (2008) miRDB: a microRNA target prediction and functional annotation database with a wiki interface. RNA 14:1012-1017.

White BC, Sullivan JM, DeGracia DJ, O'Neil BJ, Neumar RW, Grossman LI, Rafols JA, Krause GS (2000) Brain ischemia and reperfusion: molecular mechanisms of neuronal injury. J Neurol Sci 179:1-33.

Yang D, Sun Y, Hu L, Zheng H, Ji P, Pecot CV, Zhao Y, Reynolds S, Cheng H, Rupaimoole R, Cogdell D, Nykter M, Broaddus R, Rodriguez-Aguayo C, Lopez-Berestein G, Liu J, Shmulevich I, Sood AK, Chen K, et al. (2013) Integrated analyses identify a master microRNA regulatory network for the mesenchymal subtype in serous ovarian cancer. Cancer Cell 23:186-199.

Yang J, Chen L, Yang J, Ding J, Li S, Wu H, Zhang J, Fan Z, Dong W, Li X (2014) MicroRNA-22 targeting CBP protects against myocardial ischemia-reperfusion injury through anti-apoptosis in rats. Mol Biol Rep 41:555-561.

Ye Y, Hu Z, Lin Y, Zhang C, Perez-Polo JR (2010) Downregulation of microRNA-29 by antisense inhibitors and a PPAR-gamma agonist protects against myocardial ischaemia-reperfusion injury. Cardiovasc Res 87:535-544.

Zhang X, Wang X, Zhu H, Zhu C, Wang Y, Pu WT, Jegga AG, Fan GC (2010) Synergistic effects of the GATA-4-mediated miR-144/451 cluster in protection against simulated ischemia/reperfusion-induced cardiomyocyte death. J Mol Cell Cardiol 49:841-850.

Zhao F, Xuan Z, Liu L, Zhang MQ (2005) TRED: a Transcriptional Regulatory Element Database and a platform for in silico gene regulation studies. Nucleic Acids Res 33:D103-107.

C-Editor: Zhao M; S-Editors: Wang J, Li CH; L-Editors: Deusen AV, Wysong S, Qiu Y, Song LP; T-Editor: Jia Y

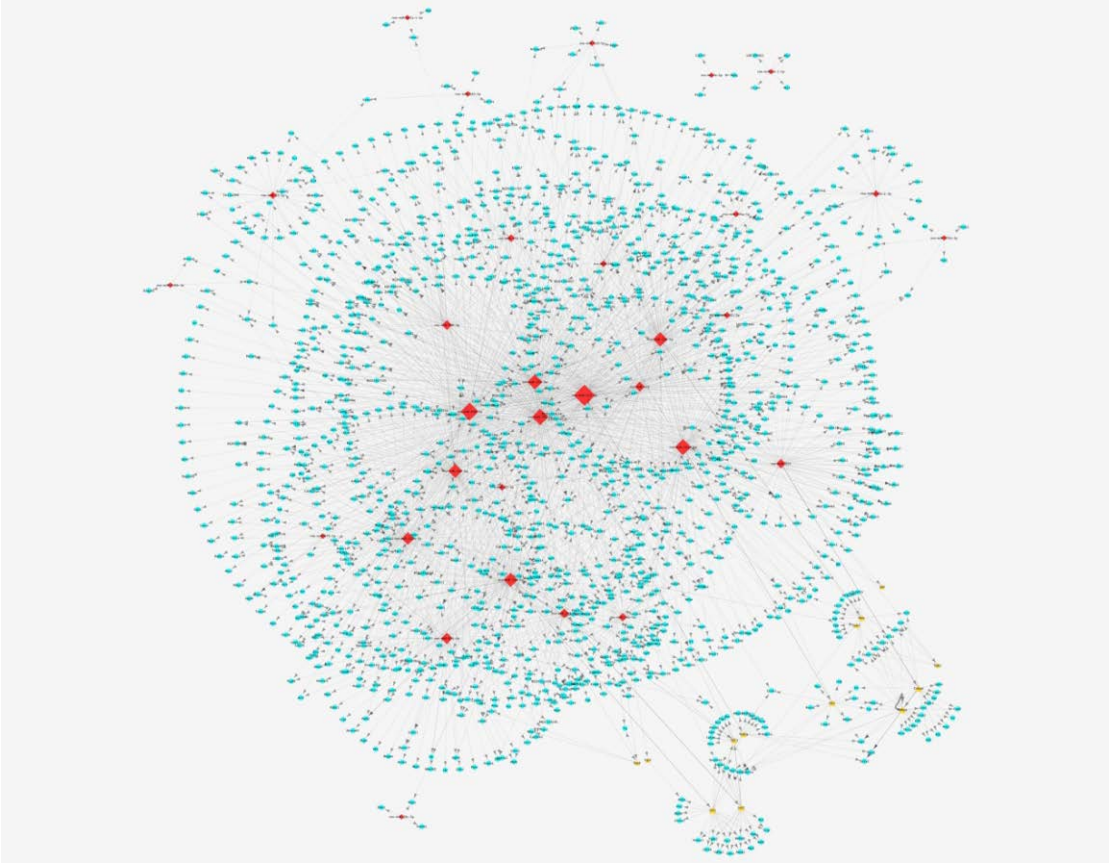

Additional Figure 1 Putative miRNA-TF regulatory patterns in SCIRI for up-regulated miRNAs in the 48-hour group.

The blue circles represent the miRNA-target genes. The yellow triangles represent the TFs. The red diamonds represent the differentially expressed miRNAs with predicted target genes. TF: Transcription factors; SCIRI: spinal cord ischemia-reperfusion injury.

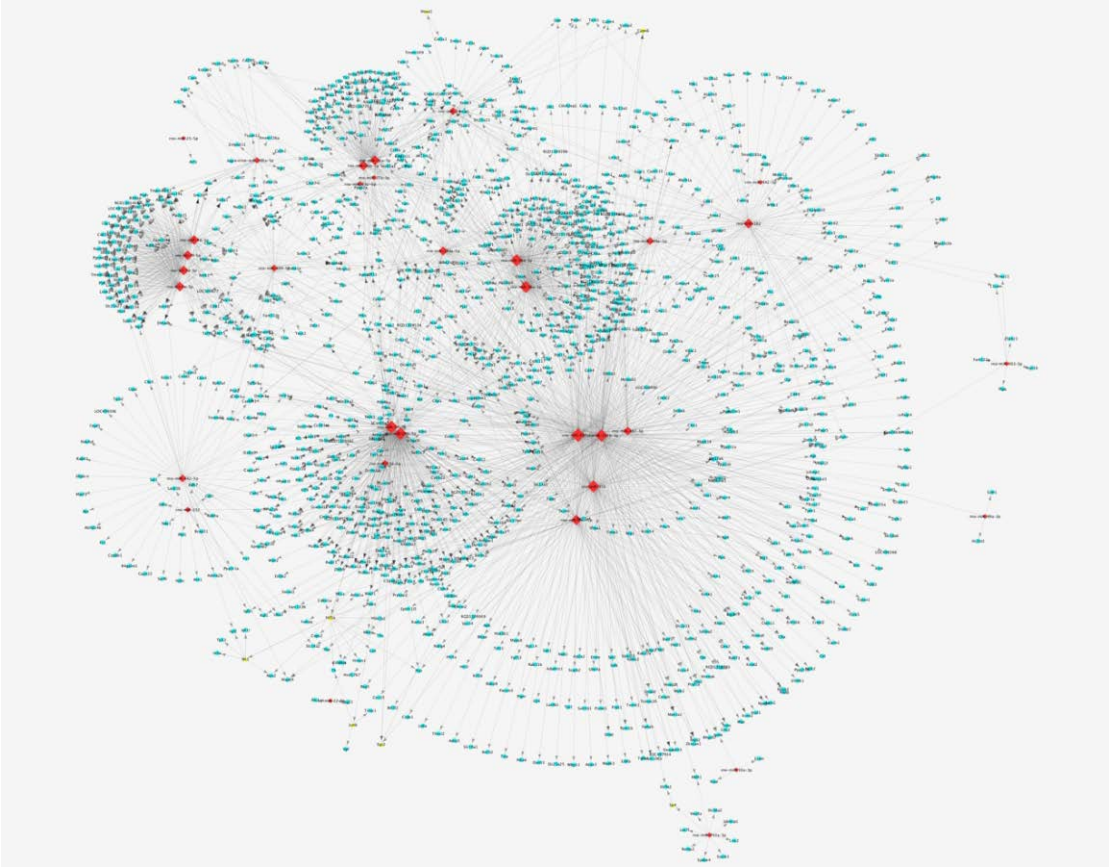

Additional Figure 2 Putative miRNA-TF regulatory patterns in SCIRI for down-regulated miRNAs in the 48-hour group.

The blue circles represent the miRNA-target genes. The yellow triangles represent the TFs. The red diamonds represent the differentially expressed miRNAs with predicted target genes. TF: Transcription factors; SCIRI: spinal cord ischemia-reperfusion injury.